ELSEVIER

Polymer 41 (2000) 8931–8940

polymer

www.elsevier.nl/locate/polymer

Shear-enhanced crystallization in isotactic polypropylene Part 2. Analysis of the formation of the oriented "skin"

G. Kumaraswamy[a], R.K. Verma[a], A.M. Issaian[a], P. Wang[a], J.A. Kornfield[a,*], F. Yeh[b], B.S. Hsiao[b], R.H. Olley[c]

[a]*Division of Chemistry and Chemical Engineering, California Institute of Technology, 210-41 Pasadena, CA 91125, USA*
[b]*Department of Chemistry, State University of New York, Stony Brook, NY 11974-3400, USA*
[c]*J.J. Thompson Physical Laboratory, University of Reading, Whiteknights, Reading RG6 2AF, UK*

Received 18 October 1999; received in revised form 13 February 2000; accepted 16 February 2000

Abstract

In-situ synchrotron wide angle X-ray diffraction (WAXD) was used to follow crystallization in a polydisperse isotactic polypropylene during and after a brief interval of shear under isothermal conditions. A specific flow history was selected from the range that induces a highly oriented skin core morphology (Kumaraswamy G, Issaian AM, Kornfield JA. Macromolecules 1999;32:7537.). At the chosen crystallization temperature ($T_{cryst} = 141$°C, characteristic time for quiescent crystallization, $t_Q \sim 10^4$ s), crystalline WAXD peaks emerge during the brief interval of shear ($\sigma_w = 0.06$ MPa, $t_s = 12$ s) showing a highly oriented fiber-like diffraction pattern; primary lamellae with *c*-axis orientation were present, along with their associated crosshatched daughter lamellae. The crystallinity grew rapidly during the first 100 s ($\sim 10^{-2} t_Q$) after cessation of shear, and very slowly after that. Further, for the first 1200 s, the orientation distribution did not change from that generated during the shear pulse. Ex-situ transmission electron microscopy showed a characteristic skin-core morphology with a thin skin region consisting of oriented crystallites near the walls of the shear device, adjacent to weakly anisotropic spherulites farther from the walls. This indicates that the in-situ WAXD at the early stages of crystallization arose mainly from crystallites in the oriented skin. The skin consisted of densely nucleated thread-like line structures from which α-phase crystalline lamellae radiate. The spacing between the row nuclei in the skin increases as a function of distance from the wall of the shear device. Our data suggest that the lamellae grow from a central thread until they impinge at about 100 s to form the dense crystalline structure in the skin.

Keywords: Isotactic polypropylene; Skin core morphology; Shear-induced crystallization

1. Introduction

Experiments that monitor the earliest stages of flow-enhanced crystallization provide valuable clues regarding the microscopic origin of the effects of flow on the overall crystallization kinetics and morphology. Considering the world market for polyolefins alone, there is enormous commercial value in understanding the development of semicrystalline morphology during and after flow. Such understanding can potentially enable the design of processing strategies guided by insight into the interplay between macromolecular flow dynamics and crystallization. For example, while the role of flow in generating the row nucleated crystals had been recognized [2,3], it was physical insight into the nature of transient structure development that led Keller and coworkers [4] to develop a route to high modulus polyethylene fibers with superior thermal and mechanical properties. By decreasing the subcooling as the polymer crystallized after extrusion, they were able to generate fibers having an interlocked "shish-kebab" morphology of tapering interdigitated lamellae leading to exceptional performance. A detailed understanding of the fundamentals of structure development during processing remains elusive despite a vast literature [5–11] that examines the effect of changing resin composition (polymer characteristics and/or additives) or processing variables on specific material properties. Most experiments that examine row nucleated structures mimic the high strain and strain rates typical of polymer processing operations, but the complicated thermal and flow history experienced by a polymer make it difficult to infer the molecular variables that control the semicrystalline morphology that develops.

Recently, model "short term" shearing experiments have been devised by Janeschitz-Kriegl and coworkers [12–15] wherein a polymer is subjected to processing-like shear

* Corresponding author. Fax: + 1-626-568-8743.
E-mail address: jak@cheme.caltech.edu (J.A. Kornfield).

0032-3861/00/$ - see front matter
PII: S0032-3861(00)00236-6

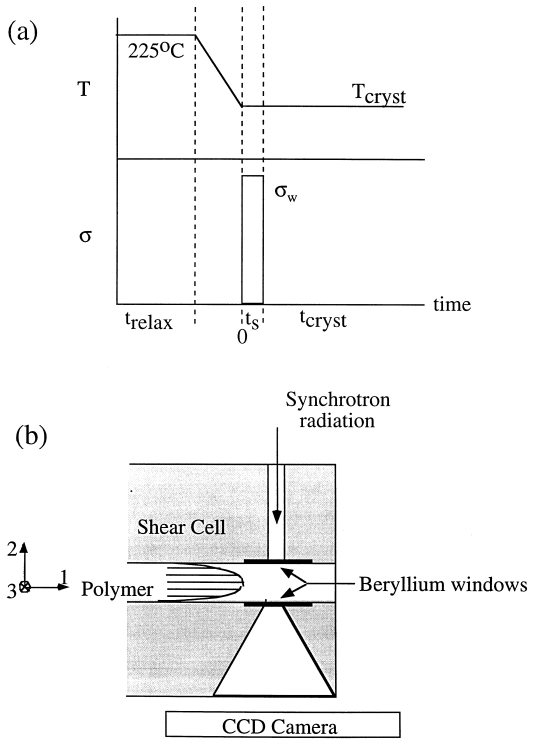

Fig. 1. (a) The experimental protocol used in our experiments subjects the polymer to a well defined, controlled thermal and flow history (see text). The thermal treatment (top graph) prior to the imposition of the box-like shear pulse (lower graph) ensures that the polymer is fully relaxed and isothermal at T_{cryst} (see text). (b) Schematic of the shear cell used for in-situ synchrotron X-ray WAXD. The beryllium windows are flush with the flow channel. The flow (1), velocity gradient (2) and vorticity (3) axes are as indicated in the figure. Light propagates down the gradient direction (2) in all in-situ optical experiments.

conditions for a brief, controlled interval under isothermal conditions (Fig. 1a). A fully relaxed initial condition—that completely erases prior thermal and flow history—is created by filling the flow channel at a high temperature, above the equilibrium melting point, then cooling to the desired crystallization temperature, T_{cryst}, after the melt is fully relaxed and any residual crystallites have been melted. The desired crystallization temperature is chosen such that the quiescent crystallization time is on the order of hours. After thermal equilibration, the polymer is subjected to a brief, box-like transient shear stress (Fig. 1a) and the development of structure is monitored during shear and after the cessation of flow.

This approach eliminates the thermal transients and gradients that make it difficult to isolate the effects of flow in experiments that mimic commercial processing. A well defined flow condition is imposed: the fluid elements that move into the observation window experience only a pressure driven channel flow, the previous flow history having been erased by the thermal treatment. Fountain flow effects are also absent as there is no free surface as in mold filling. The imposition of a brief pulse of shear (brief in comparison to the time scale for crystallization at that temperature) minimizes the reorientation of crystallites in the flow field. These experiments access processing-like stresses and deformation rates (beyond the capabilities of conventional rheometers) and reproduce some of the salient morphological features observed during injection molding, while imposing well defined thermal and flow histories.

Short term shearing studies of a typical Ziegler–Natta isotactic polypropylene showed that row nucleated structures are generated by shearing and that the nonlinear decrease in the crystallization time followed a power law dependence on the shearing time and imposed wall strain rate [12,13]. Liedauer et al. [12] proposed a phenomenological model to explain these observations: they conjectured that shear led to the activation of point like nuclei in the polymer and assigned an arbitrary shear rate dependence to the rate of formation of these nuclei. Thread-like precursors aligned in the flow direction were then hypothesized to emanate from these point nuclei under the influence of sustained shear. Crystallization proceeded from these line nuclei to give rise to crystallites oriented with their chain axis in the flow direction. This “Avrami-like” model is similar to the row-nucleated model for oriented crystallization in polymers developed by Keller and Machin [16] which postulates that rowlike structures are generated in the flow direction allowing lamellar “kebabs” to develop in a plane perpendicular to flow. While these models qualitatively capture the phenomenological aspects of row-nucleated crystallization, several questions remain unexplored: What are the factors that control nucleation of these “shish-kebabs”? How is growth affected by flow history? What determines the growth geometry and inter-feature spacing? To answer these questions, model experiments similar to those of Janeschitz-Kriegl [12] are required that allow monitoring of structure development at all the length scales and over all the time scales of interest.

We have adopted the short-term shearing protocol and designed a new instrument (Fig. 1b) that expands the range of methods that can be applied to observe structure formation during these experiments and allows us to quench the sample at the end of the experiment for ex-situ examination [17]. The compact design of our instrument allows us to transport it to a synchrotron source for in-situ SAXS and wide angle X-ray diffraction (WAXD) studies.

We have previously reported rheo-optical observations [1] of the effect of shearing on the crystallization of a Ziegler–Natta isotactic polypropylene, PP-300/6 ($M_w \sim 300,000$ g/mol, polydispersity index, PDI ~ 6–8, pentad content [mmmm] ~ 96%, melt flow index = 12 dg/min at 230°C/2.16 kg load; according to information from the manufacturer, PP-300/6 contains thousand-ppm levels of antioxidants and light stabilizers, but no additives that have a significant effect on crystal nucleation). These studies [1] reveal the range of conditions that induce highly oriented morphology in the skin. At $T_{cryst} = 141$°C and $\sigma_w = 0.06$ MPa, the time for the sample to become turbid decreases dramatically from about 10^4 s for quiescent

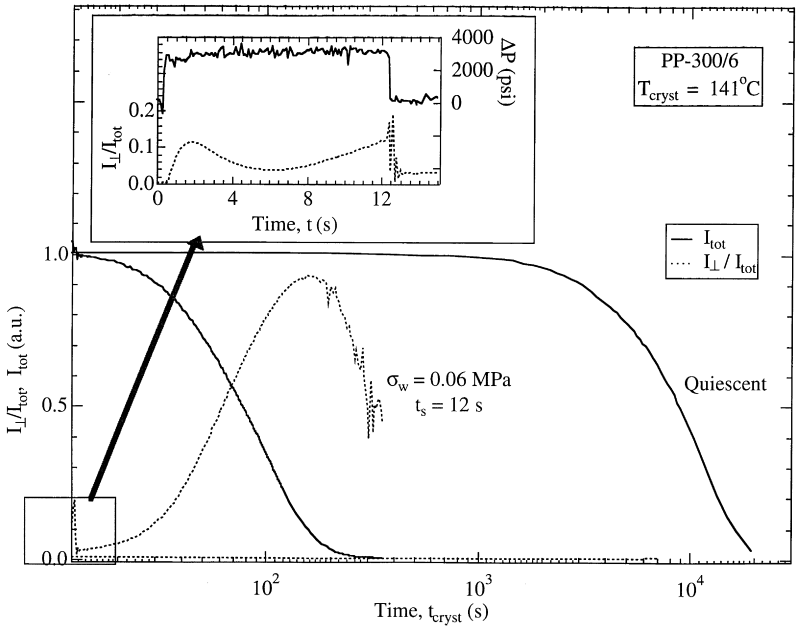

Fig. 2. The imposition of shear ($\sigma_w = 0.06$ MPa, $t_s = 12$ s) leads to a dramatic decrease in the time taken for PP-300/6 to crystallize at 141°C as can be seen from the time taken for the intensity of light transmitted through the polymer, I_{tot} (solid curves), to drop. Further, the intensity transmitted through the sample when viewed between crossed polarizers, $I_\perp/I_{tot}$ "goes over orders" for shear enhanced crystallization, indicating that highly oriented crystallites are formed. The formation of an unusual birefringent feature during the imposition of shear (inset) is a prerequisite for oriented crystallization after cessation of flow.

crystallization to $\sim 10^2$ s for shearing durations $t_s \geq 5$ s (Fig. 2). For a shearing time of $t_s = 12$ s, a strong birefringence grows as the polymer crystallizes: the normalized intensity of light transmitted through the sample examined between cross polarizers ($I_\perp/I_{tot}$) increases, indicating that highly oriented crystallites are formed (Fig. 2). This behavior correlates with the formation of an unusual upturn in ($I_\perp/I_{tot}$) observed *during* shear which does not decay to zero even after cessation of flow, indicating formation of a long-lived oriented structure that we seek to identify using WAXD (Fig. 2, inset). Under these conditions, ex-situ investigations reveal the formation of a skin-core morphology in the sample, with oriented crystallites in the skin region and a spherulitic structure in the core. Polarized optical microscopy (Fig. 4c and d in Kumaraswamy et al. [1]) indicates that the skin layer extends to about 55 μm from the walls of the flow cell. The skin is birefringent for sections viewed in the 1-2 plane, but is isotropic in the 2-3 plane (See Fig. 1). Thus, the skin shows uniaxial symmetry about the flow axis.

In this paper, we examine the transient development of the oriented skin ($T_{cryst} = 141$°C for $\sigma_w = 0.06$ MPa and $t_s = 12$ s in PP-300/6). We present in-situ synchrotron WAXD data and ex-situ TEM micrographs that show that (i) crystallites appear very rapidly ($10^{-3}\, t_Q$ at 141°C) during the shear pulse, (ii) these crystallites have a fiber-like orientation distribution (parent lamellae with chains along the flow direction and the cross hatched daughter lamellae) even at the earliest times that WAXD is detected, (iii) most of the crystallization in the skin region takes place in the first 100 s, the same time taken for the sample to turn turbid, and (iv) the morphology of the skin consists of parent lamellae that radiate out from threads along the flow direction consistent with the model of Liedauer et al. [12].

2. Experimental

In-situ studies of the evolution of crystalline structure are carried out using a range of optical probes (birefringence and turbidity measurements with visible light; SAXS and WAXD using synchrotron radiation). A piston is used to drive polymer held in a reservoir through a flow cell having a slit with a rectangular cross section of 5×0.5 mm^2 (Fig. 1b). This aspect ratio is large enough to generate a nearly two-dimensional flow profile over the central portion of the cell where the measurements are made. The pressure drop across the flow cell is measured using a pressure transducer and is used to calculate the wall shear stress experienced by the polymer. Wall shear stresses, σ_w, of up to 0.1 MPa can be imposed with rise/fall times on the order of 20 ms to give a box-like shear stress profile (Fig. 1a). Synchrotron radiation is incident on the polymer through ports in the sample cell sealed with 300 μm thick beryllium windows. A conical aperture on one side of the sample cell allows us to observe diffraction to angles (2θ) of up to $\approx 35°$.

In the experiment described in this paper, the flow cell was initially held at $T_{relax} = 225$°C and filled with polymer melt from the reservoir (Fig. 1b). We have previously

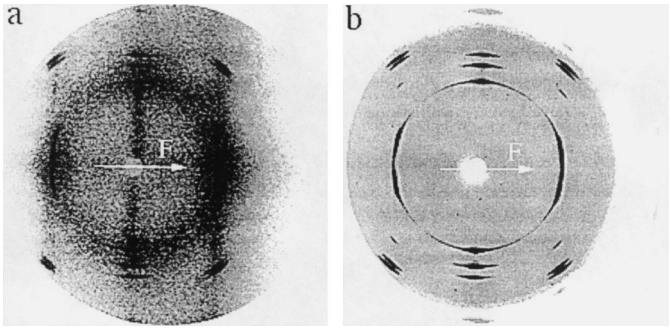

Fig. 3. In-situ two-dimensional WAXD patterns obtained as PP-300/6 crystallizes under shear ($T_{cryst} = 141°C$, $\sigma_w = 0.06$ MPa, $t_s = 12$ s). The flow direction is horizontal. (a) is obtained by acquiring data for 10 s as the polymer is being sheared and (b) is the diffraction pattern obtained at $t_{cryst} = 1200$ s using an acquisition time of 40 s. The data have been normalized for acquisition time; the normalized intensity at the 040 peak is 85 for (a) relative to 518 for (b).

established [1] that holding at this elevated temperature for 5 min erases the memory of the filling process and melts any residual crystallites. The cell is then cooled to the crystallization temperature, $T_{cryst} = 141°C$ and held isothermal thereafter (Fig. 1a). Temperature stability was maintained to within $\pm 0.3°C$ using a combination of cartridge heaters controlled by a feedback controller and a high temperature bath recirculating silicone oil through channels cut into the flow cell. Once the sample was at T_{cryst}, the relaxed, subcooled polymer melt was extruded at $\sigma_w = 0.06$ MPa for a shearing time of $t_s = 12$ s.

In-situ synchrotron WAXD was used to follow the development of semicrystalline morphology in PP-300/6 during and after the cessation of shear. Experiments were carried out at beamline X27C of the National Synchrotron Light Source (NSLS), Brookhaven National Laboratory using an X-ray wavelength of 1.307 Å. For ease of alignment, the entire shear device was placed on a translation stage allowing us to move it perpendicular to the incident X-ray beam. Data was acquired using a liquid-cooled CCD (MAR-CCD) with a resolution of 1024×1024 pixels (pixel size = 128.8 μm). The detector was placed about 16 cm from the sample cell. The scattering angles were calibrated using an α-alumina NIST standard.

Ex-situ optical and electron microscopy were used to study the morphology of the sample extracted from the shear device at $T_{cryst} = 1200$ s and quenched into cold water [17]. Samples were prepared for TEM using the permanganic etching method developed by Bassett and Olley [18] or a modification of the same procedure [19]. In both cases, a smooth surface in the 1-2 plane is created by a diamond knife and then brought into relief by etching; the resulting topography is replicated using cellulose acetate, which is then shadowed and coated with carbon. The cellulose acetate is then removed by solvent extraction, and the replica is examined using transmission electron microscopy. In the original procedure [18], etching is performed by vigorously shaking the sample with a 0.7% w/v solution of potassium permanganate in a mixture of 2 volume parts concentrated sulphuric acid and 1 part phosphoric acid for 30 min and the shadowing is performed using platinum–carbon. In the modified procedure [19], etching is performed by vigorously shaking the sample in a 1% solution of potassium permanganate in a mixture of 10 volume parts concentrated sulphuric acid, 4 parts orthophosphoric acid (85%), and 1 part water for 60 min and the shadowing is performed using tantalum–tungsten. Compared with the previous method, the modified etchant is better for revealing fine lamellar detail.

3. Results

The evolution of crystallinity and its transient orientation distribution in PP-300/6 sheared at $T_{cryst} = 141°C$ for 12 s at a wall shear stress of 0.06 MPa is monitored using in-situ synchrotron WAXD; since the observed scattering represents an average across a spatially heterogeneous sample, interpretation of the X-ray results is facilitated by TEM images of the micro- and nano-scale morphology. We begin by examining the two-dimensional WAXD patterns generated in-situ as the polymer crystallizes.

Shearing PP-300/6 at a wall shear stress of 0.06 MPa for 12 s at $T_{cryst} = 141°C$ gives rise to a strongly oriented fiber-like diffraction pattern (Fig. 3). This pattern appears during shear (Fig. 3a) and is essentially unchanged in shape at much longer times ($t_{cryst} = 1200$ s, Fig. 3b). A very weak near-isotropic ring is observed for the 110 peak at 1200 s, resulting from a small fraction of crystallites that are not highly oriented. The bimodal [20–22] diffraction patterns in Fig. 3a and b are characteristic of the monoclinic crystalline unit cell of the α-phase. This distinctive pattern is unique to isotactic polypropylene and is attributed to the crystallographic branching of "daughter" lamellae growing epitaxially with their *a*- and *c*-axes parallel to the *c*- and *a*-axes of the "parent" lamellae respectively [18,23–28]. The diffraction patterns in Fig. 3a and b may be interpreted in view of the uniaxial symmetry evident ex-situ by polarized optical microscopy [1], and can be explained in terms of parent lamellae that have their chain (*c*) axis aligned along the flow direction with a uniaxial distribution about that direction and the *b* axes of parent and daughter lamellae parallel

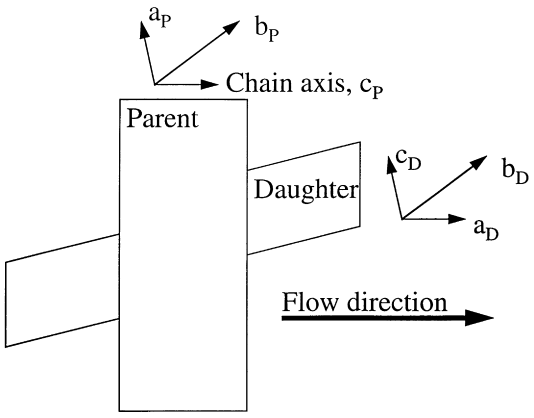

Fig. 4. A schematic model for the alignment of the parent and daughter lamellae in the oriented crystallites that explains the diffraction patterns in Fig. 3 (see text).

(Fig. 4). It has been suggested in the literature [29,30] that the imposition of shear on isotactic polypropylene leads to an increased tendency to form the β crystal phase. However, in our experiments, the hexagonal diffraction pattern characteristic of the β phase [31,32] is not observed. Further, we do not observe scattering from either the γ-phase [30] or the mesomorphic phase [33,34].

Two-dimensional WAXD patterns (such as those in Fig. 3) can be circularly averaged to generate plots of diffracted intensity as a function of the scattering vector $q = (4\pi/\lambda)\sin\theta$, where λ is the wavelength of the radiation used and 2θ is the scattering angle (Fig. 5). Well established unit cell parameters for the α form of isotactic polypropylene ($a = 6.65$ Å, $b = 20.96$ Å, $c = 6.5$ Å, $\beta = 99°80$) [31,35] can be used to index the crystalline reflections as indicated in Fig. 5. The absence of a clearly resolved feature at $q = 1.14$ Å^{-1} (where the 300 peak of the β phase is expected to appear) indicates that no detectable β crystals are present. At $T_{cryst} = 141°C$, crystalline WAXD peaks appear by the end of ten seconds of shear (our time resolution in this data set is limited by the acquisition time, which was set to 10 s; other experiments at this T_{cryst} and σ_w show that WAXD peaks emerge during the first 5 s of shearing; note that at this T_{cryst}, the quiescent crystallization time by optical methods is on the order of 10^4 s, Fig. 2). The peaks grow rapidly until $\approx$ 100 s (Fig. 5), after which they "saturate" and grow relatively slowly (Fig. 5, inset). This accords well with our in-situ rheo-optical turbidity data [1] (i.e. the time scale for the crystallinity to "saturate" corresponds to the time for the sheared polymer to become turbid).

This "saturation" behavior is also seen in the azimuthal scans at the 110 peak (Fig. 6), which show a rapid initial increase in amplitude followed by a more gradual change. Furthermore, since the parent and daughter peaks are resolved in azimuthal angle, their respective full widths at half maximum (FWHM) can be used to qualitatively assess the orientation distribution of the two populations (Fig. 7). The FWHM for the parent and daughter peaks do not change significantly with time (Fig. 7) indicating that the orientation distribution of anisotropic crystallites set up during shear (12 s) does not change substantially up to 1200 s. The fraction of daughter crystals relative to the parent population is proportional to the ratio of the areas under the respective peaks [36]. This area ratio is also roughly constant (Fig. 7) with time up to 1200 s. Although a true quantitative measurement of FWHM and area would require

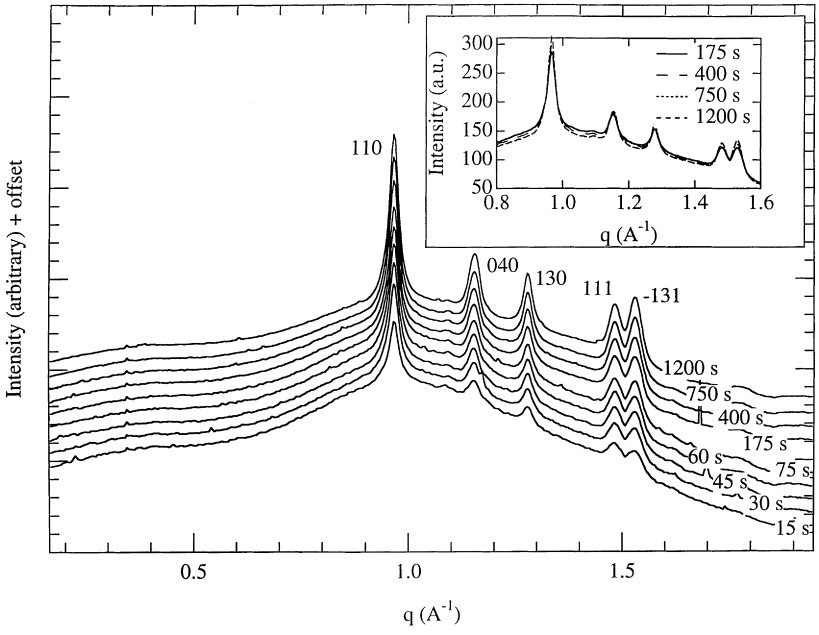

Fig. 5. As PP-300/6 crystallizes, the evolution of crystallinity can be monitored using circularly averaged "powder" patterns, normalized for data acquisition time. The data is vertically offset for clarity. The inset shows scans at $t_{cryst} = 175$, 400, 750 and 1200 s without an offset.

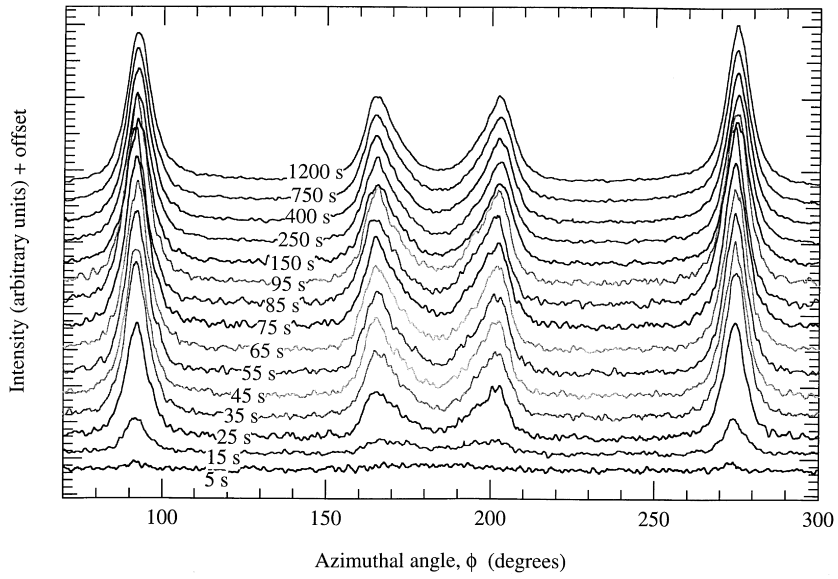

Fig. 6. Azimuthal scans at the 110 peak show the change in the crystallinity and the orientation distribution of crystallites as PP-300/6 crystallizes. The data is scaled for acquisition time and vertically offset for clarity.

X-ray images taken at several tilting angles, the results here are sufficient to indicate that the characteristic polypropylene cross-hatched morphology is developed as the shish-kebabs are formed during flow, and continues to grow after cessation of flow.

The sheared sample is quenched into cold water at about 1200 s, long after the time for the rapid growth in crystallinity to "saturate". The sample is then sectioned and the 1-2 surface is examined by TEM using the method developed by Bassett and Olley [18]. A low magnification image shows an oriented morphology in the skin layer that transitions sharply into a region that has anisotropic spherulitic structures (Fig. 8). At greater depths, the spherulites become progressively more isotropic and larger in size. The skin region extends for about 60 μm (the grid bar in Fig. 6 obscures part of the skin). We infer that the oriented structures in the skin have uniaxial symmetry since polarized optical microscopy [1] reveals the skin is birefringent in the 1-2 plane and isotropic in the 2-3 plane. Thus, the skin is comprised of row-nucleated structures extending in the

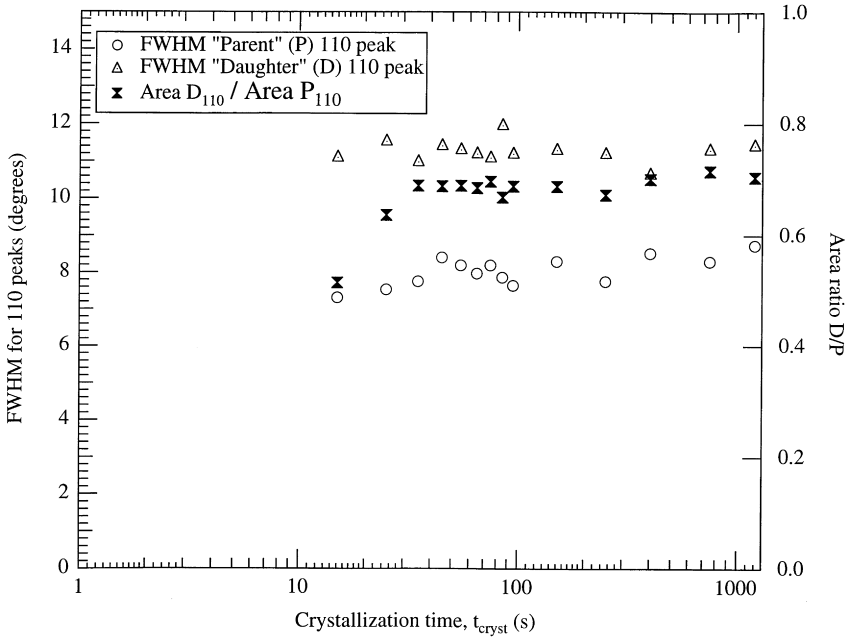

Fig. 7. Characteristics of the orientation distributions: the full width at half maximum (FWHM) for parent and daughter peaks and the ratio of the areas under daughter and parent peaks as a function of time. The first data point is at 15 s.

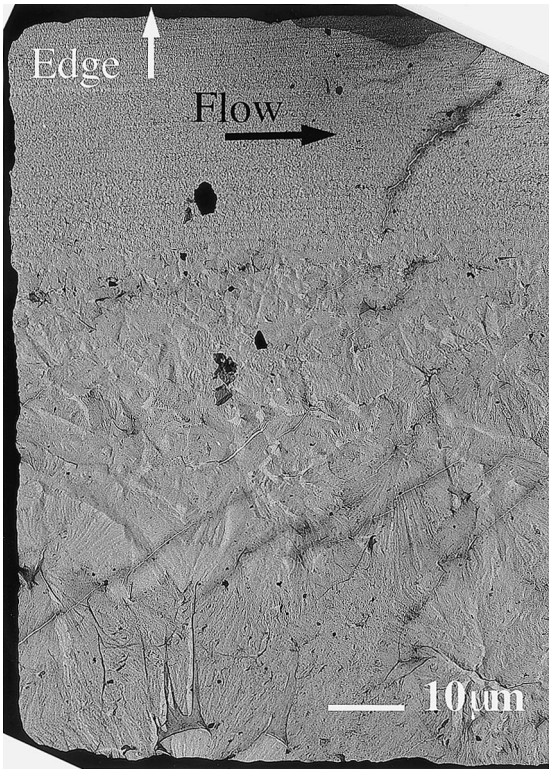

Fig. 8. A low magnification TEM image that shows the skin-core structure in shear crystallized PP-300/6. Note that the transition from the oriented skin region to the less oriented region appears sharp even at this magnification. The modified etching procedure was used to prepare the replica for this TEM image (see Section 2).

flow direction. Similar structures have been observed in the skin layers in the experiments of Liedauer et al. [12] and also by White and Bassett [37]. The spacing between the line-like structures, d_{line}, observed increases from the wall inwards. The region of the skin near the walls was examined at a higher magnification (Fig. 9) to determine an inter-line spacing of $d_{line} \approx 260$ nm in the outer 15 μm of the oriented skin. Due to the dense crystalline morphology in this region, the detailed structure of the line-like features could not be observed. In a region of the skin further away from the wall, near the boundary with the less oriented region (Fig. 10), the lines were less dense ($d_{line} \approx 700$ nm). The lamellae that grow perpendicular to the line-like features are clearly evident and show an interlamellar spacing of about 30 nm. Cross hatched lamellar branches can also be observed in some regions.

4. Discussion

The present X-ray and electron microscopy experiments aim to answer specific questions raised by rheo-optical observations made during flow and subsequent crystallization of the present sample under these specific conditions. Prior rheo-optical results (Fig. 2) indicate that a long-lived, oriented structure is induced during shear of PP-300 at the present conditions of T_{cryst}, σ_w and t_s (Fig. 2, inset); however, birefringence measurements do not enable identification of this structure (e.g. discriminating between anisotropic density fluctuations, an oriented rotator phase, or a particular crystalline morphology of iPP). The observed correlation between the induction of this type of anisotropic structure *during* shear and the growth of anisotropic crystallites after cessation of flow manifested in a large birefringence suggests some sort of templating of the orientation of the crystallites formed after flow by the long-lived structure created during flow; however, the optical data cannot suggest the mechanism of templating. The

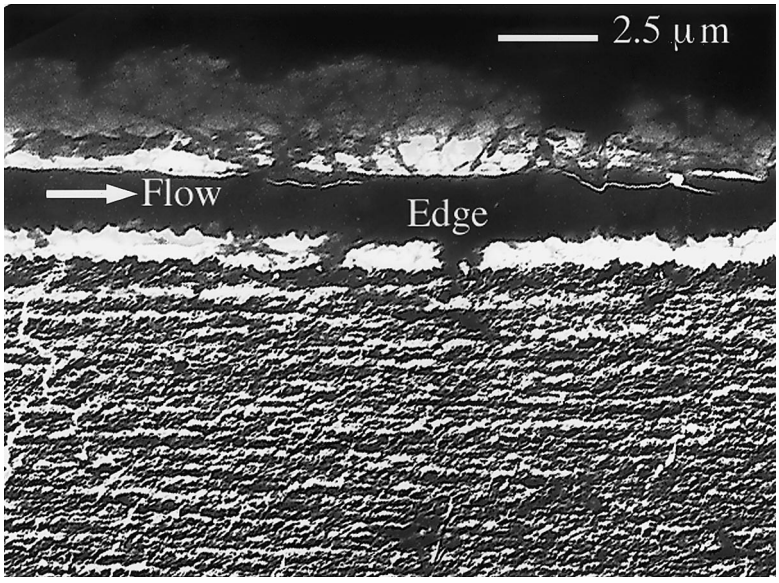

Fig. 9. A magnified image of the oriented skin near the edge of the sample. The inter-line spacing, d_{line}, is about 260 nm in this image. The Bassett and Olley etching procedure was used to prepare the replica for this TEM image (see Section 2).

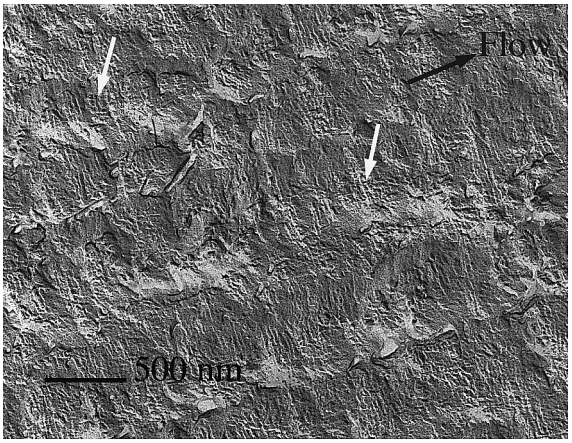

Fig. 10. A magnified view of the oriented skin far from the sample edge, near the transition to unoriented structures shows details of the lamellar structures in the skin. The primary lamellae are perpendicular to the flow direction. The inter-line spacing, $d_{line} \approx 700$ nm. The white arrows indicate regions where cross hatching is apparent. The Bassett and Olley etching procedure was used to prepare the replica for this TEM image (see Section 2).

development of turbidity, sufficient to effectively extinguish the transmitted beam of light in the rheo-optical experiments occurs at approximately 100 s; this indicates the development of a crystalline microstructure that strongly scatters visible light, but does not provide information on the morphology of this microstructure or the extent of crystallization. Once the transmitted beam is extinguished, no further information can be gained using these in-situ optical measurements. Ex-situ polarized optical microscopy gives some information on the region of the sample that might be responsible for the optical anisotropy observed during the first 100 s. The 55 μm-thick oriented skin that is observed in the resulting images provides an upper bound on the thickness of the region that contributes to the large birefringence observed in real time during crystallization; however, polarized optical microscopy does not allow us to more quantitatively describe the orientation distribution of the crystallites, nor the morphological arrangement of the semicrystalline microstructure within the oriented layer.

In-situ WAXD data presented here show that crystallinity develops during shear, indicating that the birefringent precursor observed in the rheo-optical experiments is crystalline isotactic polypropylene. The crystals that grow after shear cessation retain the orientation distribution that develops during shear indicating that the crystalline precursor formed during flow templates crystal growth after shear cessation. After the initial rapid increase in the crystallinity, the WAXD peaks "saturate" at about 100 s. This accords well with the time scale for turbidity manifested in the rheo-optical experiments. Ex-situ TEM and optical microscopy [1] provide us with a morphological interpretation of the WAXD "saturation" and rheo-optical turbidity. "Saturation" of WAXD occurs due to the impingement of lamellae that are nucleated on uniaxial thread-like precursors in the skin, growing out radially. The spacing between these thread-like structures (260–700 nm) is on the order of the wavelength of the light used in the rheo-optical experiments explaining why they scatter strongly and cause the development of strong turbidity in ~O(100 s). In this section, we discuss these observations and their implications for a geometric model of shear-enhanced crystallization.

One of the remarkable features of our data is that the orientation distribution of crystallites growing from the thread-like precursors that formed during shear does not change even after the cessation of shear. The uniaxial orientation in the skin layer leads to a separation of the diffraction from parent and epitaxial daughter crystallites for some reflections, which can be exploited to determine the ratio of the individual crystal populations and their orientations. Branched daughter peaks develop at the same time as the parent peaks (within the resolution of our experiment) and grow in proportion as the sample crystallizes.

Electron micrographs show that the less oriented layer that is observed adjacent to the oriented "skin" has a very different lamellar orientation distribution from the skin (Fig. 8). Therefore, the observation that the orientation distribution of the crystallites remains essentially unchanged during the first 1200 s implies that little crystallization occurs in the less oriented regions on a timescale of O(10^3 s). That only a small amount of crystallinity develops in the core regions over this time (which experience very low shear strain rates)[1] accords well with our quiescent in-situ WAXD and turbidity measurements [1,38]. Thus, we interpret the optical and X-ray signals during the first 1200 s as arising predominantly from the outermost 60 μm skin region near each wall of the shear cell. The "saturation" of the crystallinity after 100 s suggests that crystallization of these outer layers reaches very nearly its ultimate extent at 141°C within approximately 100 s.

A physical explanation for the rapid "completion" of the skin (in one hundredth of t_Q) and the correlation between the turbidity and WAXD crystallization times (both ~100 s) emerges from the morphology of the skin seen in the electron micrographs. The spacing between the shear lines in the skin increases from about 260 nm near the wall of the flow cell to about 700 nm near the inner boundary. The time taken for crystals growing radially from lines separated by 700 nm to impinge can be estimated to be around 105 s using a literature value for the linear growth rates of αiPP ≈ 0.2 μm/min at $T \approx 140$°C (obtained from quiescent DSC studies of polymers with similar levels of tacticity [30,39] to PP-300/6). The quiescent value for the linear growth velocity provides a good approximation because most of the growth occurs after cessation of flow and the

[1] Nonlinear viscoelastic data obtained using a capillary rheometer indicate that PP-300/6 is shear thinning with a power law exponent of 0.38. Under pressure driven flow, a blunted velocity profile develops with high strain rates near the wallsand much lower strain rates as we move away from the wall.

change in nucleation geometry (thread-like) does not alter growth velocity [37]. In addition, prior studies of the effects of shear on polymer crystallization found the growth velocity was unchanged [40]. An impingement time of 105 s agrees remarkably well with the duration of the initial rapid growth in crystallinity from our WAXD data, and suggests that the thread-like precursors generated during shear nucleate the growth of oriented crystals in the skin. Even though the growth velocity of lamellae in row structures is not discernibly different from that in spherulites, the simple geometrical factor of growing from row nuclei means that the cylindrical semicrystalline structures that result will tend to occupy a larger volume fraction—even when the row nucleation is sparse and of similar spacing to that of the spherulites [37]. These crystals then grow at their quiescent growth rate until they impinge.

The resemblance between the oriented crystallites observed in injection molding or fiber extrusion experiments and the shear experiments described here and in the literature [12] is striking. The crystalline structures observed in the skin region in our samples are similar to the row-nucleated shish-kebab structures typically observed in the "shear zone" in injection molded samples [10,21,41–43]. It is commonly believed that the fibrillar nuclei for these oriented crystals are created by the extensional fountain flow at the advancing flow front as the mold is filled. The oriented crystallites in our experiments also resemble those present in high modulus polyethylene fibers studied by Keller and coworkers among others [3,4,44]. In their studies, oriented crystal precursors were produced in the extrusion direction due to extensional flow imposed on polyethylene; these served as row nuclei for lamellae that grow out from the central precursor until they impinge, leading to the formation of high modulus materials. Since extensional flows are excluded by the short term shearing experimental protocol, these experiments, in accord with earlier work by Liedauer et al. [12], demonstrate that shear is sufficient for the formation of these oriented crystallites. The fact that thread-like precursors can be generated by various flows and that there is a sharp skin-to-core transition (Fig. 8) suggests that their formation is governed by a "critical" configurational distortion of the melt [16,45–48].

Our experiments argue for rheological control of the formation of the oriented skin: The temperature dependence of creation of the oriented precursors follows that of the melt rheology—in stark contrast to the temperature dependence of quiescent crystallization [1]. In addition, the skin has uniaxial symmetry (ex-situ optical micrographs [1]) with row-nucleated structures with "shish" along the flow direction (TEM presented here). Taken together, these results indicate that chain elongation in the flow direction generated during shear governs the morphological and kinetic transition to skin formation. In rheological terms, the primary normal stress difference plays a dominant role, in accord with the strong nonlinearity of flow-induced effects. Further, this suggests a molecular perspective on the role of chain length polydispersity that strongly affects the generation of skin-core morphologies [49]. When flow is imposed on a polymer with a broad distribution of molecular weights, high overall deformation rates can be accessed since the average chain length and, consequently, the viscosity are modest. This deformation rate is fast compared to the relaxation time of the longest chains, causing their conformation to become particularly distorted. These chains, which become elongated in the flow direction, appear to play a critical role in the cascade of events that leads to the row-nucleated structures.

The data presented here support the physical picture captured by the phenomenological model of Liedauer et al. [12] Thread-like precursors oriented in the flow direction are generated during shear. These precursors lead to the formation of oriented lamellae with their chain axes along the flow direction that grow radially from these lines until they impinge. In isotactic polypropylene, the parent lamellae are also accompanied by the associated daughter lamellae. However, the molecular variables that control the density of these lines, their generation and relaxation rates, and the "critical" shear stress that leads to oriented growth are not fully understood. Experiments with model systems that are underway in our laboratory hold promise for providing important clues regarding the molecular basis of the effects of flow on crystallization.

5. Conclusions

By observing the growth of the oriented skin induced by a brief "pulse" of shear, we not only see that the crystallization of the skin is essentially completed in roughly 1% of the quiescent crystallization time (for the present conditions), but further gain insight into how this rapid "completion" occurs. In a matter of seconds, thread-like precursors are generated during shear in the high stress regions (less than 55 μm from the wall where $\sigma_{12} > 0.047$ MPa); these thread-like precursors develop with a high density (a mere 250–700 nm apart). Primary lamellae are nucleated on these threads and forced to grow radially (with little non-crystallographic splaying) due to the geometric constraint imposed by the dense lateral packing of lamellae. Consequently, the orientation distribution created during flow persists to the point where lamellae growing from adjacent thread-like precursors impinge. Thus, we have been able to observe in real time the events that have been hypothesized to explain the row-nucleated morphology since Keller and Machin [16].

By the end of the shear pulse (12 s), the relative degree of crystallinity in the skin reaches 20% of its saturated value, which is reached in 100 s; thereafter it remains nearly constant to over 1000 s. The saturated degree of crystallinity reflects a densely crystallized, fully impinged structure. The time for impingement accords with literature values of the quiescent growth velocity.

The strong orientation of the crystallites exposes the interesting fact that cross-hatched lamellae appear almost immediately, growing simultaneously and in proportion to the parent lamellae.

Acknowledgements

We are grateful to Dr Abaneshwar Prasad (Equistar Chemical) for providing us with the polymer, PP-300/6 used in this study. We would like to acknowledge financial support from Procter and Gamble, the Cargill-NIST ATP, the Schlinger fund and NSF (DMR 9901403). This research was carried out (in part) at the National Synchrotron Light Source, Brookhaven National Laboratory, which is supported by the US Department of Energy, Division of Materials Sciences and Division of Chemical Sciences under contract number DE-AC02-98CH10886. We would like to thank Dr Lonny Berman, NSLS, Brookhaven National Laboratory, for the use of the MAR-CCD.

References

[1] Kumaraswamy G, Issaian AM, Kornfield JA. Macromolecules 1999;32:7537.
[2] Binsbergen FL. Nature 1966;211:516.
[3] Southern JH, Porter RS. J Appl Polym Sci 1970;14:2305.
[4] Odell JA, Grubb DT, Keller A. Polymer 1978;19:617.
[5] Mencik Z, Fitchmun DR. J Polym Sci: Polym Phys 1973;11:973.
[6] Fitchmun DR, Mencik Z. J Polym Sci: Polym Phys 1973;11:951.
[7] Peterlin A. Colloid Polym Sci 1987;265:357.
[8] Gupta RK, Auyeung KF. J Appl Polym Sci 1987;34:2469.
[9] Ulcer Y, Cakmak M. Polymer 1997;38:2907.
[10] Fujiyama M, Wakino T, Kawasaki Y. J Appl Polym Sci 1988;35:29.
[11] Fujiyama M, Wakino T. J Appl Polym Sci 1991;43:57.
[12] Liedauer S, Eder G, Janeschitz-Kriegl H, Jerschow P, Geymayer W, Ingolic E. Int Polym Proc 1993;8:236.
[13] Liedauer S, Eder G, Janeschitz-Kriegl H. Int Polym Proc 1995;10:243.
[14] Jerschow P, Janeschitz-Kriegl H. Rheol Acta 1996;35:127.
[15] Jerschow P, Janeschitz-Kriegl H. Int Polym Proc 1997;12:72.
[16] Keller A, Machin MJ. J Macromol Sci B 1967;1:41.
[17] Kumaraswamy G, Verma RK, Kornfield JA. Rev Sci Instrum 1999;70:2097.
[18] Bassett DC, Olley RH. Polymer 1984;25:935.
[19] Shahin MM, Olley RH, Blissett MJ. J Polym Sci Part B: Polym Phys 1999;37:2279.
[20] Andersen PG, Carr SH. J Mater Sci 1975;10:870.
[21] Clark ES, Spruiell JE. Polym Engng Sci 1976;16:176.
[22] Masada I, Okihara T, Murakami S, Ohara M, Kawaguchi A, Katayama KI. J Polym Sci: Polym Phys 1993;31:843.
[23] Padden Jr. FJ, Keith HD. J Appl Phys 1966;37:4013.
[24] Padden Jr. FJ, Keith HD. J Appl Phys 1973;44:1217.
[25] Binsbergen FL, Lange BG, M D. Polymer (London) 1968;9:23.
[26] Lovinger AJ. J Polym Sci: Polym Phys 1983;21:97.
[27] Lotz B, Wittmann JC. J Polym Sci: Polym Phys 1986;24:1541.
[28] Norton DR, Keller A. Polymer 1985;26:704.
[29] Wenig W, Herzog F. J Appl Polym Sci 1993;50:2163.
[30] Karger-Kocsis J, editor. tructure and Morphology Polypropylene, vol. 1. London: Chapman and Hall, 1995.
[31] Lotz B, Wittmann JC, Lovinger AJ. Polymer 1996;22:4979.
[32] Dorset DL, Court MP, Kopp S, Schumacher M, Okihara T, Lotz B. Polymer 1998;39:6331.
[33] Natta G, Corradini P. Nuovo Cimento (Suppl.) 1960;15:40.
[34] Corradini P, Petraccone V, Rosa CD, Guerra G. Macromolecules 1986;19:2699.
[35] Jones AT, Aizlewood JM, Beckett DR. Makromol Chem 1964;75:134.
[36] Dean DM, Rebenfeld L, Register RA, Hsiao BS. J Mater Sci 1998;33:4797.
[37] White HM, Bassett DC. Polymer 1997;38:5515.
[38] Kumaraswamy G, Verma RK, Issaian AM, Wang P, Kornfield JA, Yeh F, Hsiao BS, Olley RH. (in preparation).
[39] Janimak JJ, Cheng SZD, Giusti PA, Hsieh ET. Macromolecules 1991;24:2253.
[40] Wolkowicz M. J Polym Sci: Polym Symp 1978;63:365.
[41] Kantz MR, Newman Jr. HD, Stigale FH. J Appl Polym Sci 1972;16:1249.
[42] Folkes MJ, Russell DAM. Polymer 1980;21:1252.
[43] Kalay G, Bevis M. J Polym Sci: Polym Phys 1997;35:265.
[44] Bashir Z, Odell JA, Keller A. J Mater Sci 1984;19:3713.
[45] Hill M, Keller A. J Macromol Sci Phys B 1971;5:591.
[46] Keller A, Kolnaar HWH. Processing of polymers. In: Meijer HEH, editor. Chapter flow induced orientation and structure formation, Vol. 18. New York: VCH, 1997.
[47] McHugh A, Guy R, Tree D. Colloid Polym Sci 1993;271:629.
[48] Bushman AC, McHugh AJ. J Appl Polym Sci 1997;64:2165.
[49] Meijer H, editor. Processing of polymers, Vol. 18. New York: VCH, 1997.